Food Research International 203 (2025) 115772

Contents lists available at ScienceDirect

Food Research International

journal homepage: www.elsevier.com/locate/foodres

Cork impact on red wine aging monitoring through ^{1}H NMR metabolomics: A comprehensive approach

Guillaume Leleu [a], Luca Garcia [b], Patricia Homobono Brito de Moura [a], Gregory Da Costa [a], Cédric Saucier [b,*], Tristan Richard [a,*]

[a] Univ. Bordeaux, Bordeaux INP, Bordeaux Sciences Agro, INRAE, OENO, UMR 1366, ISVV, 33140 Villenave d'Ornon, France
[b] SPO, Univ. Montpellier INRAE, Institute Agro, 34000 Montpellier, France

ARTICLE INFO

Keywords:
Cork stoppers
Red wine aging
^{1}H NMR metabolomics
Oxygen transfer rate

ABSTRACT

Cork stoppers have a significant impact on aging as a place of gas exchange. This study investigates the effects of different cork closures on red wines using ^{1}H NMR metabolomics approach. The objective is to understand how different cork stoppers affect the chemical evolution of wine during aging. Six Syrah wines from the Côtes du Rhône and Languedoc-Roussillon regions, matured in either steel tanks or oak barrels, were bottled with four micro-agglomerated cork stoppers. Over 24 months, wines were analyzed using ^{1}H NMR spectroscopy. Data were processed using multivariate analyses: principal component analysis (PCA), hierarchical cluster analysis (HCA), and orthogonal projections to latent structures discriminant analysis (OPLS-DA). The analyses revealed significant changes along the wine aging process. Distinct chemical signatures were identified for wines at the initial and 24-month stages. At the initial stage, wine maturation conditions, stainless steel tank or oak barrel, seem to impact wine constituents, including methanol, ethyl lactate, acetic acid, myo-inositol, and isobutanol. Finally, corks with higher oxygen transfer rate (OTR) showed higher content in acetoin, suggesting its application as an oxygenation marker of wines. The findings highlight the complex role of cork permeability in red wine aging, suggesting that the choice of cork can be strategically used to steer the aging process and enhance wine quality.

1. Introduction

Chemical analysis of wines plays a crucial role in the wine industry. It allows for quality control and authenticity verification while providing a better understanding of the chemical processes behind this beverage. Among the myriad of analytical techniques available, Nuclear Magnetic Resonance (NMR) metabolomics stands out as a powerful tool for characterizing the molecular structure and composition of wine (Cassino, Tsolakis, Bonello, Gianotti, & Osella, 2019; Le Mao, Da Costa, & Richard, 2023; López-Rituerto et al., 2022; Mascellani et al., 2021). NMR spectroscopy offers several advantages for metabolomic analysis, such as high reproducibility, and the ability to simultaneously detect a wide range of compounds without extensive sample preparation (Wishart, 2019).

The aging of red wines is a complex process in which time and environmental factors induce changes that influence the final quality of the wine. Among the factors involved in this process, the choice of closure plays a crucial role (Garcia, Martet, Suc, Garcia, & Saucier, 2024; Pons et al., 2022). As the wine ages in bottle, the cork serves as a guardian and a mediator. As the wine ages in the bottle, the cork serves as a guardian and a mediator. Cork is recognized for its ability to allow controlled oxygen exchange, benefiting the qualitative evolution of red wines. In the context of red wine aging, NMR-based metabolomics is a method that could help to study the influence of cork on the chemical evolution of wines during bottle aging.

This manuscript presents a pioneering investigation into the impact of cork closure on the aging of red wines, employing a comprehensive NMR metabolomics approach. We aim to track the biochemical changes induced by aging and cork interaction, highlighting their implications for wine quality and stability. Furthermore, these findings showed that NMR-based metabolomics appears capable of distinguishing between different winemaking protocols, such as the type of tank used.

* Corresponding authors.
E-mail addresses: cedric.saucier@umontpellier.fr (C. Saucier), tristan.richard@u-bordeaux.fr (T. Richard).

https://doi.org/10.1016/j.foodres.2025.115772
Received 31 October 2024; Received in revised form 14 January 2025; Accepted 14 January 2025
Available online 17 January 2025

2. Material and methods

2.1. Wine samples

Six red wines, all 100 % Syrah, were sourced from various wineries within the Côtes du Rhône (CR) and Languedoc-Roussillon (LR) regions (Table 1). As previously described (Garcia et al., 2024), these wines were produced using conventional winemaking methods and conserved in tanks or in oak barrels during the maturation phase. Before bottling, the free SO_2 levels were adjusted to 30 mg·L^{-1}. The wines were filled into 0.75 L Bordelaise bottles. The cork stoppers were then inserted manually using a vacuum corker randomly. Four types of micro-agglomerated cork stoppers were provided by DIAM Bouchage (Céret, France). The oxygen transfer rates (OTR) and initial oxygen rates (OIR) data for these stoppers were measured by luminescence-based technology and provided by the manufacturer (Table 1). To study the aging process, triplicates of bottles and corks were aged for 24 months at 17 °C. A total of 90 wine bottles were analyzed during the study: 18 at the initial stage before bottling (T0, 6 wines × 3 replicates) and 72 after 24 months of aging (6 wines × 4 corks × 3 replicates). Wine samples were aliquoted into 2 mL plastic vials under argon gas and conserved at –80 °C. All the analyses were performed at the same time.

2.2. NMR analysis

2.2.1. NMR sample preparation

The procedure described here follows our previous methodology (Gougeon, da Costa, Guyon, & Richard, 2019). After thawing at room temperature, the wine samples were submitted to centrifugation at 14,500 rpm for 5 min. Subsequently, 200 µL of phosphate buffer (1 M, pH 2.6) and 100 µL of deuterated water containing 0.5 mM TMSP and 7 mM Calcium Formate (FCa) were added to 700 µL of wine. The pH was then adjusted to 3.1 using a semi-automatic system (BTpH, Bruker BioSpin, Wissembourg, Germany) using 1 M DCl or NaOD solutions.

2.2.2. ^{1}H NMR analyse

^{1}H NMR spectra were collected using an Advance III spectrometer (Bruker BioSpin) operating at 500 MHz using a 5 mm ATMA BBI inverse probe with z-gradient coils and a BACS-120 autosampler using TopSpin IconNMR 3.0 software (Bruker Biospin, Karlsruhe, Germany). The measurements were performed at 300 K, without sample rotation, using TopSpin 3.6 software (Bruker BioSpin). Initial automated shimming was performed to achieve a line width at half maximum below 1 Hz for the TMSP signal. Pulse calibration was achieved before each sample analysis. Two distinct sequences were used: 1D proton spectrum with water suppression (zgpr, D1 = 15 s, AQ = 3.40 s, DS = 2, NS = 8, SW = 16 ppm, TD = 64 k) and 1D proton multi-solvent suppression through a 1D-NOESY experiment targeting water and ethanol signals (noesygpps1d, D1 = 15 s, AQ = 3.40 s, DS = 4, NS = 32, SW = 16 ppm, TD = 64 k, D8 = 100 ms).

Table 1
Wine samples and cork stoppers.

Wine	Origin	Maturation
CR1	Côtes du Rhone	Tank
CR2	Côtes du Rhone	Oak barrel
LR1	Languedoc-Roussillon	Oak barrel
LR2	Languedoc-Roussillon	Oak barrel
LR3	Languedoc-Roussillon	Tank
LR4	Languedoc-Roussillon	Oak barrel
Cork	OIR (mg)	OTR (mg/year)
D1	0.77 ± 0.03	0.30 ± 0.10
D2	1.72 ± 0.25	0.90 ± 0.10
D3	1.76 ± 0.15	1.10 ± 0.10
D4	2.19 ± 0.13	1.80 ± 0.40

Subsequently, the FIDs underwent multiplication by an exponential function with a baseline broadening factor of 0.3 Hz before Fourier transformation. Manual phase correction and alignment using the TMSP signal ($\delta = 0$ ppm) were performed. Quantification of wine constituents was carried out using MestReNova 14.0.0 software (Mestrelab Research, Santiago de Compostela, Spain), employing the external Simple Mixture Analysis (SMA) module. A laboratory-developed library facilitated semi-automatic quantification of 47 metabolites (Gougeon et al., 2018; Le Mao, Da Costa, Bautista, de Revel, & Richard, 2023). Compounds affected by ethanol signal suppression were quantified using the zgpr sequence: ethanol, methanol, glycerol, succinic acid, acetic acid, lactic acid, ethyl lactate, myo-inositol, 2,3-butanediol, and isobutanol (Tables S1 and S2, in supplementary data).

2.3. Statistical analysis

The statistical analyses were conducted using SIMCA 17 software (Sartorius Stedim, Göttingen, Germany). Prior to analysis, no pre-processing steps were applied to the data. The dataset was centered and scaled to unit variance using the default procedure in SIMCA. Initially, a principal component analysis (PCA) was employed to visualize the dataset's distribution and to identify any potential outliers for exclusion from further analysis. A maximum of three principal components were used. Both explained variance (R^2) and predicted variance (Q^2) were reported for each PCA model. Hierarchical cluster analysis (HCA) was applied to the data to detect similarities between clusters. Following PCA, an orthogonal projection to latent structures discriminant analysis (OPLS-DA) was performed (Wheelock & Wheelock, 2013; Worley & Powers, 2016). The resulting analyses were visualized in a two-dimensional graph, with a Hotelling T^2 ellipse denoting the 95 % confidence zone. The quality of these analyses was assessed using R-squared (R^2) and Q-squared (Q^2) values, representing the goodness of fit and prediction quality, respectively. Cross-validation was employed to validate sample ranking in each analysis. Subsequently, a loading graph was generated to identify potential discriminating metabolites, determined by their variable importance in projection (VIP) and correlation coefficient (p-(corr)). Metabolites with VIP values greater than 1.0 and p-(corr) values exceeding 0.5 in absolute terms were considered potential discriminant compounds. Student's *t*-test was conducted to identify compounds with significant variation using XLSTAT 2022.2.1 (Addinsoft, Paris, France). For variables not conforming to a normal distribution, non-parametric Mann Whitney's test was employed.

3. Results and discussion

3.1. Wine global analyze

In this study, Syrah red wines from six different wineries and two regions (Côtes du Rhone and Languedoc-Roussillon) elaborated using two maturation procedures (tank and oak barrel) were collected (Table 1). The free SO_2 levels were adjusted before bottling. Wines were conserved in a bottle for 24 months using four different cork stoppers of increasing oxygen permeability. All wines were analyzed by NMR-based metabolomics.

In the initial stage of chemometric analysis, the distribution of each wine was examined before bottling (T0) and after 24 months of aging using multivariate analysis of NMR data extracted from zgpr spectra. This experiment quantifies ten wine constituents: ethanol, methanol, glycerol, succinic acid, acetic acid, lactic acid, ethyl lactate, myo-inositol, 2,3-butanediol and isobutanol (Table S1).

In this initial treatment, principal component analysis (PCA) was applied to the data matrix derived from analyzing all wines. PCA, being an unsupervised technique, facilitates sample clustering without prior knowledge of group membership. This method aids in visually representing data, highlighting both their similarities and disparities. The PCA score plot obtained is presented in Fig. S1, in supplementary data.

Even if an aging effect seems to appear, a clear discrimination based on the winery is observed.

To confirm this observation, the wines at the initial stage (T0) and after 24 months of aging (T1) were analyzed separately by PCA (Fig. 1A, top left and right, respectively). The first two principal components (PCs) account for 68.1 % and 56.7 % of the variability among the tested samples for T0 and T1, respectively. The results clearly indicated that each wine has its own signature at T0 and after 24 months of aging. No discrimination based on geographical origin is observable between Languedoc-Roussillon and Côtes du Rhône wines. Interestingly, the PCA score plot of the wine at T0 exhibited significant separation between wines maturated in tanks and wines maturated in oak barrels along the PC2 axis. This observation, based on the metabolites quantified on the zgpr experiments, disappears after 24 months suggesting that the wines evolve differently during bottle aging.

To maximize the separation between wines maturated in tanks and in oak barrels, supervised orthogonal projection to latent structures discriminant analysis (OPLS-DA) was applied. OPLS-DA is a supervised approach that emphasizes distinctions between two groups and identifies the variables with the greatest discriminatory capability. The OPLS-DA score plot (Fig. 1B), coupled with validation and permutation protocols, confirmed the ability to separate wines maturated in tanks and in oak barrels independently of the origin. Model performances are summarized in Fig. 1B. R^2Y and Q^2 were employed to assess the model. R^2Y indicates the goodness of fit, while Q^2 measures the goodness of prediction. Typically, a Q^2 value greater than 0.5 is deemed favorable, and a difference of less than 0.3 between R^2Y and Q^2 is recommended in metabolomics (Li et al., 2017). We achieved a satisfactory discrimination between the two wine classes, with R^2Y and Q^2 values of 0.973 and 0.942, respectively. Moreover, permutation tests (100 iterations) and CV-ANOVA were utilized to validate the model's predictive capacity and statistical significance (Yuan et al., 2020). All permuted R^2 and Q^2 values were lower than the initial ones, with the intercepts of R^2 and Q^2 values on the Y-axis being <0.5 and <0, respectively. Additionally, the p-values of CV-ANOVA were <0.05, indicating a good fit for the OPLS-DA model. Finally, model predictive performance was confirmed through classification rate (CCR) and area under the curve (AUC) values obtained from the ROC curves (100 % and 1.0, respectively).

Based on the OPLS-DA model, the discriminant compounds between tank and oak barrel maturation were identified. For this purpose, VIP and p-(corr) parameters were used (Le Mao et al., 2021). Wine constituents presenting absolute VIP and p-(corr) values greater than 1.0 and 0.5, respectively, were selected as potential markers. The identified metabolites were checked by unpaired *t*-test or Mann-Whitney's test. Only compounds with p-value < 0.05 were highlighted. Using this protocol five compounds were identified (Fig. 1C). We observe higher levels of methanol in tanks and lower levels of ethyl lactate, acetic acid, myo-inositol, and isobutanol.

Tanks and oak barrels are widely used for wine maturation (White & Catarino, 2023). Stainless-steel tanks are generally considered as inert vessels, whereas oak barrels act as active vessels due to their oxygen permeability. Methanol decrease in oak barrels compared to tanks was already observed in a previous study (Wei et al., 2020). In line with our research, Di Renzo et al. observed lower concentrations of ethyl lactate, myo-inositol, and isobutanol after maturation in stainless-steel tanks compared to oak barrels. This suggests that wine maturation in oak barrels may better facilitate fermentation, a process intricately linked to the complex chemical reactions in winemaking. Our results affirm that the final concentrations of higher alcohols are influenced by oxygenation conditions, as evidenced by the lower concentration of acetic acid after maturation in tanks, consistent with this observation.

3.2. Red wine bottle aging

Based on the zgpr experiments, the clear discrimination based on the winery is observed (Fig. S1). Consequently, each wine was analyzed separately to investigate the effect of aging.

In this second stage of the chemometrics, each wine was submitted to multivariate analysis based on the 1H NMR data extracted from zgpr and NOESY spectra. A total of 47 metabolites were identified and quantified (Tables S1 and S2) including organic acids, alcohols, amino acids, sugars, phenolics, and esters. The results of the multivariate analysis of LR1 wines were presented in Fig. 2.

Unsupervised PCA and hierarchical cluster analysis (HCA) were performed to assess clustering based on wine aging in bottle of LR1 samples (Fig. 2A, top right and middle, respectively). The first two principal components (PCs) account for 58.4 % of the variability (42.7 and 15.7 % for PC1 and PC2, respectively). Based on PCA score plot, a clear discrimination is observed between T0 and T1 samples along PC1. Interestingly, it can be noticed that a gradient appears along PC2 among the T1 wines between the samples closed with different cork stoppers. There is a clear differentiation between wines closed by D1 and D4 corks along PC2. The HCA dendrogram is consistent with the results of the PCA (Fig. 2A, top middle). Three main clusters are observed on the dendrogram corresponding to T0 wines; wines closed with D1 and D4 cork stoppers. Samples closed with D2 and D3 cork stoppers are distributed between D1 and D4 clusters.

Supervised OPLS-DA was applied to differentiate LR1 wines at the initial stage (T0) and after 24 months of aging (T1). Using the OPLS-DA model, two groups were obtained, discriminating T0 and T1 wines into the OPLS-DA score plot (Fig. 2B, top left). The validation and performance parameters of the model are reported in Table 2. The values of R^2X, R^2Y and Q^2 (0.572, 0.983 and 0.956, respectively) indicate the goodness-of-fit and predictability of the OPLS-DA model. A significant CV-ANOVA value *p*-value < 0.05, the results of permutation tests (100 times), and the AUC value of 1.0 from the ROC curves confirm the model validity and performance (Table 2). Finally, the classification rate (CCR) of 100 % indicates the predictive ability of the model.

The OPLS-DA model was employed to pinpoint the principal discriminant metabolites, utilizing VIP and p-(corr) values, with thresholds set at >1.0 and 0.5, respectively. A set of ten markers was identified and further validated through univariate statistical analysis (Fig. 2B). Only metabolites with p-value <0.05 were conserved. LR1 wines, after 24 months of aging, show a lower concentration of arabinose, xylose, catechin, epicatechin, isoamyl alcohol and myo-inositol, and a higher concentration ethyl acetate, ethyl lactate, lactic acid and tyrosol.

The same analytical protocol was applied to the remaining five wines. Unsupervised PCA was employed to observe the sample distribution within each wine set. The resulting PCA score plots clearly depicted a distinction between T0 and T1 wines following 24 months of bottle aging (Fig. S2). All wines exhibited discrimination along the first principal component, with PC1 explaining 45.1, 45.6, 42.2, 48.9, and 47.9 % of the total variance for LR2, LR3, LR4, CR1, and CR2 wines, respectively. Supervised OPLS-DA was then utilized to differentiate between T0 and T1 samples for each wine, as illustrated in Fig. S3. The quality parameters of the OPLS-DA models for each wine are presented in Table S3. Satisfactory models were achieved for bottle aging discrimination in each wine, with R^2Y and Q^2 values exceeding 0.983 and 0.913, respectively (Table S3). Furthermore, the validity of the models was confirmed by CV-ANOVA p-values below 0.05 and permutation tests. The CCR and AUC values for each wine (100 % and 1.0, respectively) underscored the robust predictability and performance of the OPLS-DA models (Table S3).

Based on OPLS-DA models, the discriminant compounds were selected. Only metabolites presenting VIP and p-(corr) values upper than 1.0 and 0.5 were selected, and p-value lower than 0.05 (Student's *t*-test or Mann Whitney's test) were highlighted. The results were summarized in the heatmap of Fig. 3. This heatmap gives a global visualization of the different aging markers identified in each wine. Green cells correspond to higher relative contents in the final wines after 24 months of aging in bottle, whereas brown cells, lower relative contents. A total of 26

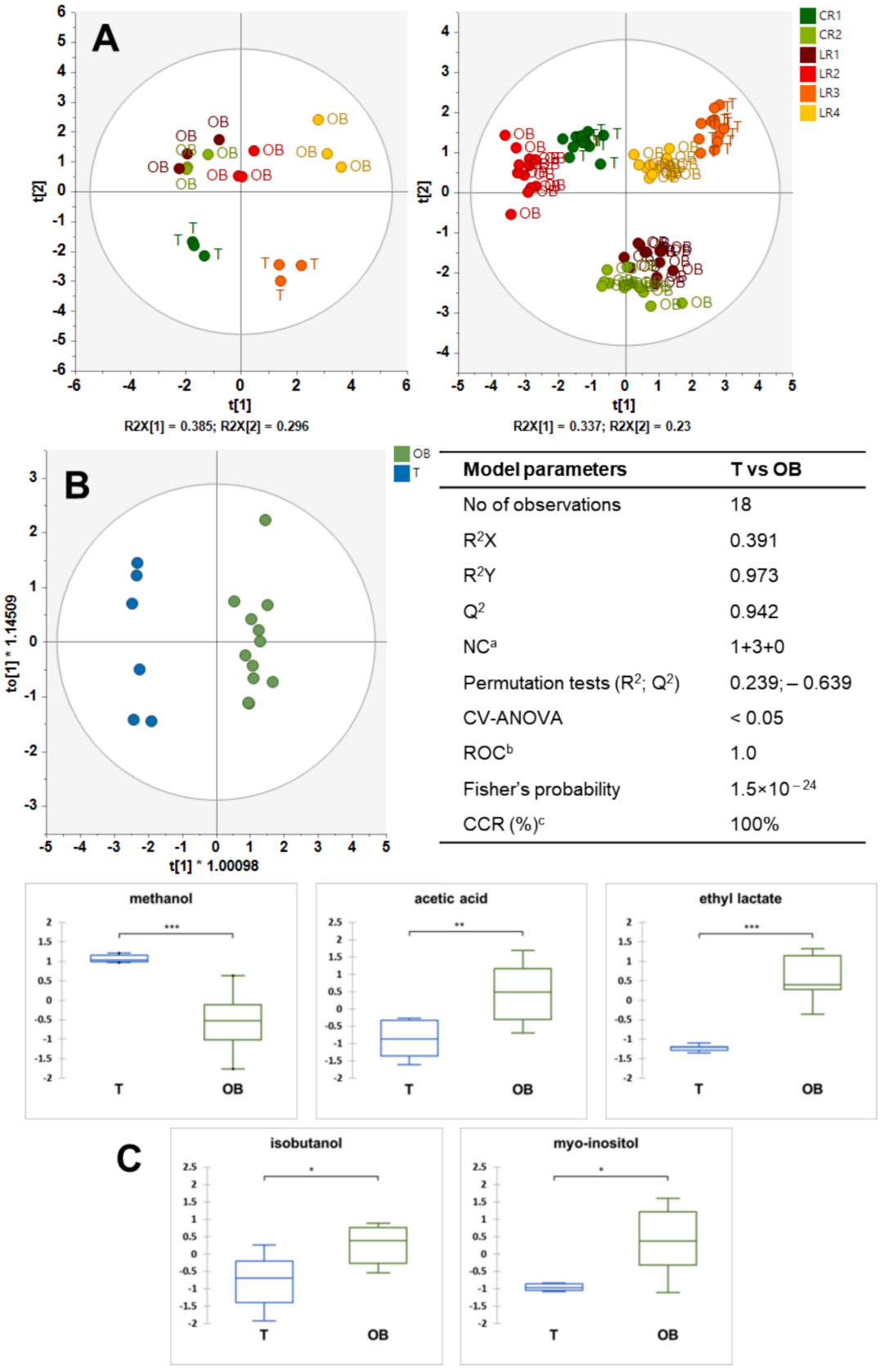

Model parameters	T vs OB
No of observations	18
R^2X	0.391
R^2Y	0.973
Q^2	0.942
NC[a]	1+3+0
Permutation tests (R^2; Q^2)	0.239; – 0.639
CV-ANOVA	< 0.05
ROC[b]	1.0
Fisher's probability	1.5×10^{-24}
CCR (%)[c]	100%

Fig. 1. Statistical analysis of wines based on the 1H NMR data extract from zgpr spectra. PCA score plot (**A**) of wines before bottling (left) and after 24 months of aging (right) in bottles (T labels: wines maturated in tanks; OB labels: wines maturated in oak barrels). Scores plot and validation parameters of the OPLS-DA model (**B**) and relative boxplot for the discriminant elements (**C**) of wines maturated in tanks (blue labels) and oak barrels (green labels) before bottling (p-value: *< 0.05; **< 0.01; ***< 0.001).

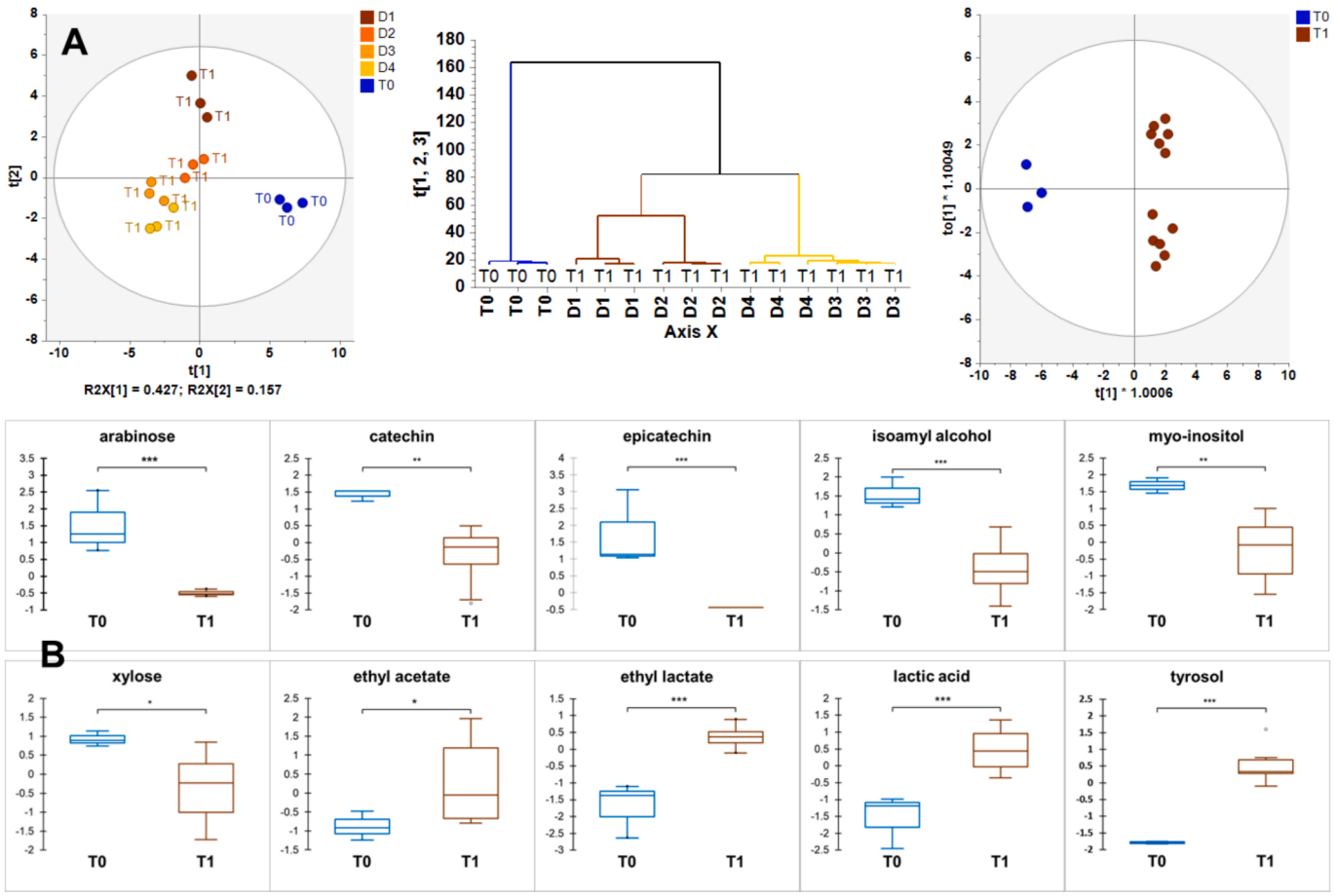

Fig. 2. Statistical analysis of LR1 wines based on the 1H NMR data. **A:** Unsupervised PCA box plot (left) and HDA box plot (center), and supervised OPLS-DA box plot (right) for wines before bottling (T0) and after 24 months of aging in bottles (T1). **B:** relative box plot for the discriminant elements of wines at T0 and T1 (p-value: *< 0.05; **< 0.01; ***< 0.001). D1: wines bottled with D1 corks; D2: wines bottled with D2 corks; D3: wines bottled with D3 corks; D4: wines bottled with D4 cork.

Table 2
Performance and validation results of PCA and OPLS-DA models of LR1 wines. Discrimination of T0 (before bottling) and T1 (after 24 months in bottles).

Model parameters	T0 vs T1	
	PCA	OPLS-DA
No of observations	15	15
R^2X	0.693	0.572
R^2Y		0.983
Q^2	0.262	0.956
NC[a]	3	1 + 1 + 0
Permutation tests (R^2; Q^2)		0.534; −0.637
CV-ANOVA		<0.05
ROC[b]		1.0
Fisher's probability		2.2×10^{-3}
CCR (%)[c]		100 %

[a] NC: No. of components.
[b] ROC: area under the (ROC) curve (AUC).
[c] CCR: correct classification rate.

metabolites were significantly impacted during bottle aging across all wines. Among these markers, some present a punctual variation for a wine, such as the lowest concentration of 2,3-butanediol and phenetyl alcohol in the CR2 wine after aging, or the highest concentration of choline in the LR2 wine (Fig. 3). Nevertheless, common features can be extracted from the analysis of all wines.

Concerning sugars, a decrease in arabinose and xylose was observed in most wines. Pentosides, such as arabinose and xylose, are not metabolized by yeast during fermentation. They are the main residual sugars in dry wines (Jackson, 2020). In wines, monosaccharides can be summited to different reactions such as oxidation, reduction, dehydration and degradation in presence of acids, or Maillard reaction with amino acids (Sanz & Martínez-Castro, 2009). All these transformations can lead to the formation of new compounds in wines including volatile compounds such as furanic derivatives or terpenes (Jackson, 2020; Sanz & Martínez-Castro, 2009). Therefore, a global decrease of monosaccharides (pentosides and hexosides) is expected during bottle aging (del Alamo, Bernal, del Nozal, & Gómez-Cordovés, 2000; Zhang et al., 2018). In contrast to these studies, no significant decline of hexosides (glucose and galactose) was observed.

Regarding phenolics, a notable reduction in catechin and epicatechin content was noted over the aging process. Catechin and epicatechin are two representative molecules of the flavan-3-ol family. They play a role in sensory attributes such as dryness and bitterness in wine, and are crucial in preserving its quality during aging (Ferrer-Gallego, Hernández-Hierro, Rivas-Gonzalo, & Escribano-Bailón, 2014). These compounds undergo diverse processes such as polymerization, copigmentation, and formation of quinone (Jackson, 2020). A decrease of monomeric flavan-3-ol is thus expected during wine aging. In contrast, we observed an increase in gallic acid during aging in most of the wines. Gallic acid holds the distinction of being one of the primary phenolic acids within red wine (Gutiérrez-Escobar, Aliaño-González, & Cantos-Villar, 2021). Along with ellagic acid, it constitutes the basic building block of hydrolysable tannins. The rise in gallic acid levels may stem from the breakdown of hydrolysable tannins such as gallo-tannins and esters of gallic acid in acidic environments, as previously described by other studies (Garde-Cerdán et al., 2022; Uzkuç, Bayhan, & Toklucu,

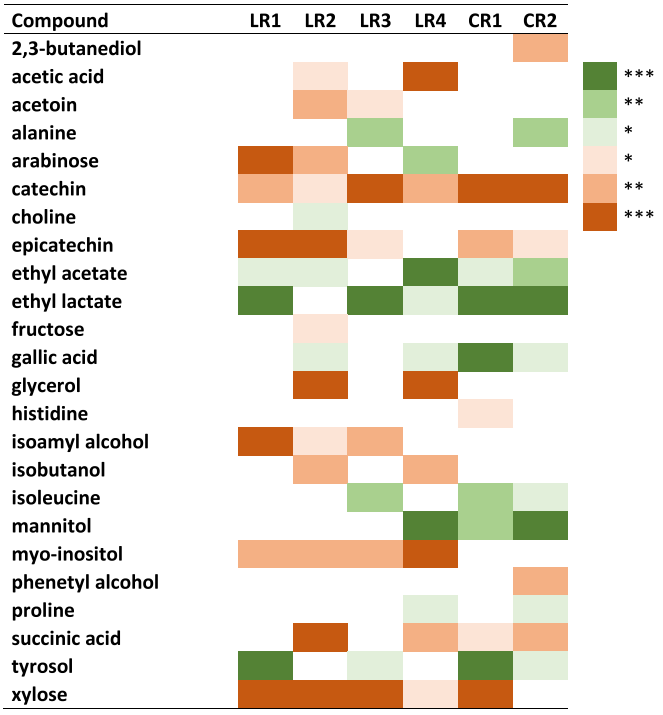

Fig. 3. Heatmap visualization of marker relative contents between T0 and T1 (24 months of aging) samples for each wines (LR1 to LR4, CR1 and CR2). Markers were identified based on VIP and p-(corr) values > 1.0 and 0.5, respectively, and p-values (*< 0.05; **< 0.01; ***< 0.001). Green cells: metabolites presenting higher concentrations at T1; brown cells: metabolites presenting higher concentrations at T1.

2022). Finally, tyrosol is augmented in several wines. This compound is mainly synthetized by yeasts. An increase of tyrosol was observed in sparkling wines due to the second fermentation in bottle (Jackson, 2020). However in red wines, the tyrosol content appears to stay relatively stable during bottle aging (Monagas, Bartolomé, & Gómez-Cordovés, 2005). More studies will be needed to explain this variation.

A global decrease of higher alcohols, such as isoamyl alcohol, isobutanol or myo-inositol, was observed in many wines. The formation of higher alcohols in wine occurs as a result of yeast fermentation, with their synthesis closely mirroring that of ethanol production (Jackson, 2020). Their concentration tends to decrease during aging due to degradation processes such as oxidation or esterification reactions (Zhang et al., 2023).

Finally, concerning organic acids and esters, we observed an increase in succinic acid and a decrease of ethyl acetate and ethyl lactate in most of the wines. Organic acids are implicated in esterification reactions. Thus a global decrease of organic acids is expected in wine during aging in bottle (Cassino et al., 2019; Giuffrida de Esteban et al., 2019). Among organic acids, only succinic acid presented significant decrease during aging. This metabolite is a common by-product of yeast metabolism (Jackson, 2020). A comparable outcome was noted during the 12-month bottle aging of Cabernet Sauvignon wine (X. K. Zhang et al., 2018). Interestingly, the rate of ester formation varies depending on the aging conditions. While hydrolysis is possible, their formation is enhanced by low pH values, high temperatures, and elevated alcohol concentrations, due to reactions between ethanol and organic acids (Shinohara & Shimizu, 1981).

3.3. Cork oxygen permeability

The effect of the different caps is more difficult to observe. The four types of micro-agglomerated cork stoppers show relatively close oxygen permeability values, with oxygen transfer rate (OTR) ranged from 0.3 (D1 stopper) to 1.8 mg/year (D4 stopper). These technical stoppers provide better control over the transfer of oxygen to and from the wine compared to traditional cork stoppers (Echave, Barral, Fraga-Corral, Prieto, & Simal-Gandara, 2021). Micro-agglomerated cork stoppers are generally used to provide controlled OTR for long-aging wines.

However, certain discrimination seems to emerge between the cork stoppers, as depicted in Fig. 2 for LR1 wines after 24 months of aging. On the PCA plot (Fig. 2A), D1 and D4 corks were distinctly separated along the PC2 axis. This finding was further supported by the HCA plot, where D1 and D4 wines formed two distinct clusters. D2 and D3 wines were shared between these two groups. Similar patterns were observed for wines LR2, LR3, and CR1 (Fig. S1, supplementary data). Conversely, LR4 and CR2 wines did not exhibit significant differentiation between the various closures.

To validate these observations, wines LR1, LR2, LR3, and CR1 underwent additional statistical analysis. The D1 and D4 conditions of these four wines were compared using multivariate statistical analyses as described earlier. PCA was employed to observe the distribution of wines, followed by OPLS-DA analysis. Upon validation of the obtained models, the main discriminating metabolites were identified based on VIP and p-(corr) values, which were further confirmed through univariate tests. Following this procedure, only wines LR1, LR2, and LR3 yielded satisfactory models (Table S4). For these three wines, clear discrimination between D1 and D4 conditions was observed after PCA (Fig. S4) along the PC1 axis (>71 % explanation of total variance). The OPLS-DA score plots are also presented in Fig. S4. The performances of the obtained models are reported in Table S4. All OPLS-DA models are satisfactory with R^2Y and Q^2 values above 0.9, CV-ANOVA values below 0.05, and satisfactory permutation tests. To identify discriminating compounds, metabolites with a VIP value greater than 1.0 and a p-(corr) value greater than 0.5 were selected. Their ability to discriminate wines was validated by univariate tests (Student's *t*-test or Mann Whitney's test). Only metabolites with a p-value below 0.5 were selected. Across all three wines, twelve metabolites show significant variation between D1 and D4 cork stoppers (Fig. 4). The observation of the results indicates that the impact of oxygenation is complex and strongly depends on the initial chemical profile of the analyzed wine.

Interestingly, it is possible to observe a lower concentration of acetoin for D1 stoppers (less oxygen-permeable) compared to the D4 stoppers (more permeable), in the three wines. Acetoin levels in wines are quite variable but can reach up to 200 mg/L with averages ranging

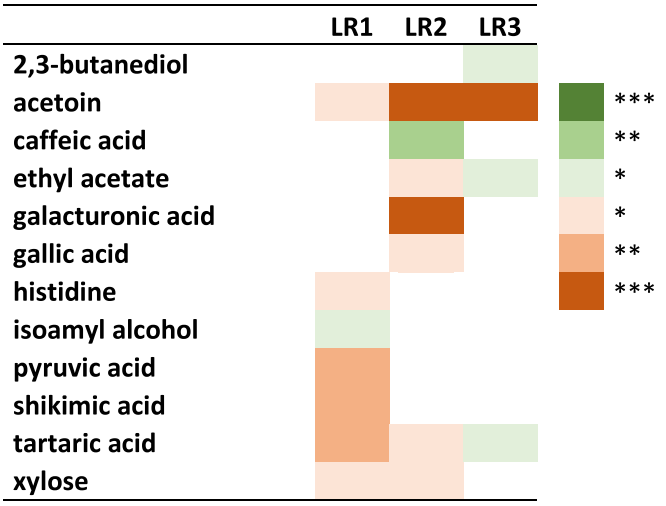

Fig. 4. Heatmap visualization of marker relative contents between D1 and D4 cork stoppers. Markers were identified based on VIP and p-(corr) values > 1.0 and 0.5, respectively, and p-values (*< 0.05; **< 0.01; ***< 0.001). Green cells: metabolites presenting higher concentrations at T1; brown cells: metabolites presenting higher concentrations at T1.

between 10 and 20 mg/L (Romano & Suzzi, 1996). Acetoin does not have a strong odorant effect; its detection threshold is higher than 100 mg/L in wines. However, it is an important compound as it is involved in the synthesis of 2,3-butanediol and diacetyl. The biosynthesis of acetoin is linked to the action of yeast during fermentation (Romano & Suzzi, 1996). Numerous parameters affect its biosynthesis, such as yeast strain, temperature, or aeration conditions. Additionally, its concentration tends to decrease towards the end of fermentation due to its reduction into 2,3-butanediol. Initially, Peynaud et al. showed that aeration conditions favour its synthesis during fermentation, its levels remaining stable in the absence of microbial activity (Peynaud, 1947). Recent studies have shown that acetoin levels in wines tend to increase during bottle aging (Han, Webb, & Waterhouse, 2019; Liu, Xing, Li, Yang, & Pan, 2016). They hypothesized that diacetyl could be reduced to acetoin during bottle aging under reductive conditions in a competitive mechanism involving acetaldehyde. In our study, we observed a significant reduction in acetoin levels during bottle aging in wines LR2 and LR3 (Fig. 3). The mechanisms of acetoin transformation thus appear to be complex and linked to the redox balance of wines. Interestingly, Han et al. found that acetoin levels after 12 months in the bottle are correlated with OTR (Han et al., 2019). The higher the OTR, the more acetoin is found in the wine. These results are consistent with our observations. Wines sealed with D4 corks contain more acetoin. Acetoin could be a marker of wine oxygenation. However, further extensive work will be necessary to confirm this observation and to better understand the complex relationships between acetoin, acetaldehyde, and 2,3-butanediol in wines.

4 . Conclusion

This study aimed to explore the influence of cork stoppers on the aging of red wines using ^{1}H NMR metabolomics approach. First, our work shows that quantitative NMR is a robust method for quantifying the main organic constituents of wine throughout the winemaking process. It offers a quick way to monitor the evolution of the wine without specific sample preparation. Multivariate analysis (PCA, HCA and OPLS-DA) followed by univariate ones reveal that maturation method, bottle aging process and cork stopper significantly impact the chemical composition of wine over time. Distinct chemical signatures related to oxygenation processes are identified for wines matured in tanks versus oak barrels, initial versus aged stages in bottle and depending on the cork stopper used.

Maturation method impacts oxygenation conditions, resulting in changes in higher alcohol content. In tank, which act as an inert vessel, higher quantities of methanol and lower levels of ethyl lactate, acetic acid, myo-inositol and isobutanol are observed compared to oak barrels, known for their oxygen permeability. During bottle aging, a decrease in specific pentosides was observed, likely linked to chemical evolution. Phenolic compounds such as catechin and epicatechin decreased, probably due to oxidative or non-oxidative mechanisms, while gallic acid content increased, possibly linked to the breakdown of hydrolysable tannins. Additionally, changes in organic acids and esters were noted, probably due to oxidation or esterification, highlighting the complex chemical transformations over time.

This study highlights the crucial role of cork stoppers' oxygen transfer rates in steering the aging process and potentially enhancing wine quality. Our findings underscore the significant impact of cork permeability on the chemical evolution of wine during aging and thus the importance of choosing the appropriate cork. Although the impact of oxygenation is complex and depends on the initial wine profile, acetoin content increased with OTR, suggesting its potential as a marker for wine oxygenation. More investigations will be necessary to confirm this observation.

Understanding the impact of corks on wine aging can inform better practices in the wine industry, benefiting both producers and consumers. This study sets the stage for further investigations into the molecular mechanisms underlying wine aging in bottle and the development of advanced strategies for wine preservation through cork stoppers.

CRediT authorship contribution statement

Guillaume Leleu: Writing – original draft, Investigation. **Luca Garcia:** Writing – review & editing, Investigation. **Patricia Homobono Brito de Moura:** Writing – review & editing, Investigation. **Gregory Da Costa:** Writing – review & editing, Investigation. **Cédric Saucier:** Writing – review & editing, Supervision, Resources, Project administration, Funding acquisition, Conceptualization. **Tristan Richard:** Writing – original draft, Supervision, Project administration, Investigation, Funding acquisition, Formal analysis, Conceptualization.

Declaration of competing interest

The authors declare that they have no known competing financial interests or personal relationships that could have appeared to influence the work reported in this paper.

Acknowledgements

This work was supported by the Bordeaux Metabolome Facility and ANR (MetaboHUB -ANR-11-INBS-0010 project and WAPNMR ANR-21-CE21-0014 project). We would also like to thank Fondation de Bordeaux (donors: Baron Philippe de Rothschild SA, Chateau Cheval Blanc, Château Lafite Rothschild, Le Domaine Clarence Dillon, Château Petrus) for their financial support. We acknowledged Diam bouchage company for funding this project and PhD grant of Luca Garcia from University of Montpellier (UM200893). Winemakers from Languedoc-Roussillon and Côtes du Rhône are thanked for allowing sampling in their cellars. Vivelys is acknowledged for its help in wine bottling.

Appendix A. Supplementary data

Supplementary data to this article can be found online at https://doi.org/10.1016/j.foodres.2025.115772.

Data availability

The data that has been used is confidential.

References

Cassino, C., Tsolakis, C., Bonello, F., Gianotti, V., & Osella, D. (2019). Wine evolution during bottle aging, studied by 1H NMR spectroscopy and multivariate statistical analysis. *Food Research International, 116*, 566–577. https://doi.org/10.1016/j.foodres.2018.08.075

del Alamo, M., Bernal, J. L., del Nozal, M. J., & Gómez-Cordovés, C. (2000). Red wine aging in oak barrels: Evolution of the monosaccharides content. *Food Chemistry, 71*(2), 189–193. https://doi.org/10.1016/S0308-8146(00)00145-X

Echave, J., Barral, M., Fraga-Corral, M., Prieto, M. A., & Simal-Gandara, J. (2021). Bottle aging and storage of wines: A review. *Molecules, 26*(3). https://doi.org/10.3390/molecules26030713

Ferrer-Gallego, R., Hernández-Hierro, J. M., Rivas-Gonzalo, J. C., & Escribano-Bailón, M. T. (2014). Sensory evaluation of bitterness and astringency sub-qualities of wine phenolic compounds: Synergistic effect and modulation by aromas. *Food Research International, 62*, 1100–1107. https://doi.org/10.1016/j.foodres.2014.05.049

Garcia, L., Martet, E., Suc, L., Garcia, F., & Saucier, C. (2024). Analysis of targeted phenolic ageing markers in Syrah red wines during bottle ageing: Influence of cork oxygen transfer rate. *Food Chemistry, 443*, Article 138491. https://doi.org/10.1016/j.foodchem.2024.138491

Garde-Cerdán, T., Sáenz de Urturi, I., Murillo-Peña, R., Iribarren, M., Marín-San Román, S., Rubio-Bretón, P., & Pérez-Álvarez, E. P. (2022). Bottle aging affected aromatic and phenolic wine composition more than yeast starter strains. *Applied Sciences, 12*(9), 4478.

Giuffrida de Esteban, M. L., Ubeda, C., Heredia, F. J., Catania, A. A., Assof, M. V., Fanzone, M. L., & Jofre, V. P. (2019). Impact of closure type and storage temperature on chemical and sensory composition of Malbec wines (Mendoza, Argentina) during

aging in bottle. *Food Research International, 125*, Article 108553. https://doi.org/10.1016/j.foodres.2019.108553
Gougeon, L., da Costa, G., Guyon, F., & Richard, T. (2019). 1H NMR metabolomics applied to Bordeaux red wines. *Food Chemistry, 301*, Article 125257. https://doi.org/10.1016/j.foodchem.2019.125257
Gougeon, L., Da Costa, G., Le Mao, I., Ma, W., Teissedre, P. L., Guyon, F., & Richard, T. (2018). Wine analysis and authenticity using 1H-NMR metabolomics data: Application to Chinese wines. *Food Analytical Methods, 11*(12), 3425–3434. https://doi.org/10.1007/s12161-018-1310-2
Gutiérrez-Escobar, R., Aliaño-González, M. J., & Cantos-Villar, E. (2021). Wine polyphenol content and its influence on wine quality and properties: A review. *Molecules, 26*(3), 718.
Han, G., Webb, M. R., & Waterhouse, A. L. (2019). Acetaldehyde reactions during wine bottle storage. *Food Chemistry, 290*, 208–215. https://doi.org/10.1016/j.foodchem.2019.03.137
Jackson, R. S. (2020). Chapter 6 - Chemical constituents of grapes and wine. In R. S. Jackson (Ed.), *Wine Science* (fifth ed., pp. 375–459). Academic Press. https://doi.org/10.1016/B978-0-12-816118-0.00006-4.
Le Mao, I., Da Costa, G., Bautista, C., de Revel, G., & Richard, T. (2023). Application of 1H NMR metabolomics to French sparkling wines. *Food Control, 145*, Article 109423. https://doi.org/10.1016/j.foodcont.2022.109423
Le Mao, I., Da Costa, G., & Richard, T. (2023). 1H-NMR metabolomics for wine screening and analysis. *OENO one, 57*(1), 15–31. https://doi.org/10.20870/oeno-one.2023.57.1.7134
Le Mao, I., Martin-Pernier, J., Bautista, C., Lacampagne, S., Richard, T., & Da Costa, G. (2021). 1H-NMR metabolomics as a tool for winemaking monitoring. *Molecules, 26*(22), 6771. https://doi.org/10.3390/molecules26226771
Li, C.-Y., Song, H.-T., Wang, X.-X., Wan, Y.-Y., Ding, X.-S., Liu, S.-J., Dai, G.-L., Liu, Y.-H., & Ju, W.-Z. (2017). Urinary metabolomics reveals the therapeutic effect of HuangQi Injections in cisplatin-induced nephrotoxic rats. *Scientific Reports, 7*(1), 3619. https://doi.org/10.1038/s41598-017-03249-z
Liu, D., Xing, R.-R., Li, Z., Yang, D.-M., & Pan, Q.-H. (2016). Evolution of volatile compounds, aroma attributes, and sensory perception in bottle-aged red wines and their correlation. *European Food Research and Technology, 242*(11), 1937–1948. https://doi.org/10.1007/s00217-016-2693-1
López-Rituerto, E., Sørensen, K. M., Savorani, F., Engelsen, S. B., Avenoza, A., Peregrina, J. M., & Busto, J. H. (2022). Monitoring of the Rioja red wine production process by 1H-NMR spectroscopy. *Journal of the Science of Food and Agriculture, 102*(9), 3808–3816. https://doi.org/10.1002/jsfa.11729
Mascellani, A., Hoca, G., Babisz, M., Krska, P., Kloucek, P., & Havlik, J. (2021). 1H NMR chemometric models for classification of Czech wine type and variety. *Food Chemistry, 339*, Article 127852. https://doi.org/10.1016/j.foodchem.2020.127852
Monagas, M., Bartolomé, B., & Gómez-Cordovés, C. (2005). Evolution of polyphenols in red wines from Vitis vinifera L. during aging in the bottle. *European Food Research and Technology, 220*(3), 331–340. https://doi.org/10.1007/s00217-004-1109-9
Peynaud, E. (1947). Le 2,3-butyleneglycol, l'acetylmethylcarbinol et le diacetyle dans les vins. *Bulletin International du Vin, 193*, 16–19.
Pons, A., Lavigne, V., Suhas, E., Thibon, C., Redon, P., Loisel, C., & Darriet, P. (2022). Impact of the closure oxygen transfer rate on volatile compound composition and oxidation aroma intensity of merlot and cabernet sauvignon blend: a 10 year study. *Journal of Agricultural and Food Chemistry, 70*(51), 16358–16368. https://doi.org/10.1021/acs.jafc.2c07475
Romano, P., & Suzzi, G. (1996). Origin and Production of Acetoin during Wine Yeast Fermentation. *Applied and Environmental Microbiology, 62*(2), 309–315. https://doi.org/10.1128/aem.62.2.309-315.1996
Sanz, M. L., & Martínez-Castro, I. (2009). Carbohydrates. In M. V. Moreno-Arribas & M. C. Polo (Eds.), *Wine Chemistry and Biochemistry* (pp. 231-248). New York, NY: Springer New York. doi: 10.1007/978-0-387-74118-5_12.
Shinohara, T., & Shimizu, J.-I. (1981). Formation of ethyl ester of main organic acids during aging of wine and indications of aging. *Nippon Nōgeikagaku Kaishi, 55*(8), 679–687. https://doi.org/10.1271/nogeikagaku1924.55.679
Uzkuç, N. M.Ç., Bayhan, A., & Toklucu, A. K. (2022). Phenolics and color components of young Cabernet Sauvignon wines: Effect of spontaneous fermentation and bottle storage. *European Food Research and Technology, 248*(2), 393–401. https://doi.org/10.1007/s00217-021-03884-x
Wei, X., Francoise, U., Qin, M., Chen, Q., Li, Y., Sun, X., & Fang, Y.-L. (2020). Effects of different fermentation and storage conditions on methanol content in Chinese spine grape (Vitis davidii Foex) wine. *CyTA - Journal of Food, 18*(1), 367–374. https://doi.org/10.1080/19476337.2020.1737238
Wheelock, Å. M., & Wheelock, C. E. (2013). Trials and tribulations of 'omics data analysis: Assessing quality of SIMCA-based multivariate models using examples from pulmonary medicine. *Molecular BioSystems, 9*(11), 2589–2596. https://doi.org/10.1039/c3mb70194h
White, W., & Catarino, S. (2023). How does maturation vessel influence wine quality? A critical literature review. *Ciència Téc. Vitiv., 38*(2), 128–151.
Wishart, D. S. (2019). NMR metabolomics: A look ahead. *Journal of Magnetic Resonance, 306*, 155–161. https://doi.org/10.1016/j.jmr.2019.07.013
Worley, B., & Powers, R. (2016). PCA as a practical indicator of OPLS-DA model reliability. *Current Metabolomics, 4*(2), 97–103. https://doi.org/10.2174/2213235X04666160613122429
Yuan, Z.-Y., Li, J., Zhou, X.-J., Wu, M.-H., Li, L., Pei, G., Chen, N.-H., Liu, K.-L., Xie, M.-Z., & Huang, H.-Y. (2020). HS-GC-IMS-based metabonomics study of Baihe Jizihuang Tang in a rat model of chronic unpredictable mild stress. *Journal of Chromatography B, 1148*, Article 122143. https://doi.org/10.1016/j.jchromb.2020.122143
Zhang, D., Wei, Z., Han, Y., Duan, Y., Shi, B., & Ma, W. (2023). A review on wine flavour profiles altered by bottle aging. *Molecules, 28*(18). https://doi.org/10.3390/molecules28186522
Zhang, X. K., Lan, Y. B., Zhu, B. Q., Xiang, X. F., Duan, C. Q., & Shi, Y. (2018). Changes in monosaccharides, organic acids and amino acids during Cabernet Sauvignon wine ageing based on a simultaneous analysis using gas chromatography-mass spectrometry. *Journal of the Science of Food and Agriculture, 98*(1), 104–112. https://doi.org/10.1002/jsfa.8444